

M.T. Kartel^{1,2}, V.V. Lobanov², E.M. Demyanenko², Wang Bo¹,
A.G. Grebenyuk², O.S. Karpenko²

SORPTION OF MOLECULAR HYDROGEN ON THE GRAPHENE-LIKE MATRIX DOPED BY N- AND B-ATOMS

¹ Ningbo University of Technology
No 55-155 Cui Bai Road, Ningbo, 315016, China

² Chuiko Institute of Surface Chemistry of National Academy of Sciences of Ukraine
17 General Naumov Str., Kyiv, 03164, Ukraine, E-mail: nikar@kartel.kiev.ua

The regularities of interaction of hydrogen molecules with graphene-like planes, where two carbon atoms are replaced by nitrogen or boron atoms, have been studied by the methods of quantum chemistry (DFT, B3LYP, 6-31G**). To take into account the dispersion contributions to the energy of formation of intermolecular complexes that occur during the formation of adsorption supramolecular structures, Grimme's dispersion correction is used - D3. To study the effect of the size of a graphene-like cluster on the energy of molecular hydrogen chemisorption, polyaromatic molecules (PAM) are used of pyrene, coronene and that consisting of 54 carbon atoms, as well as their nitrogen- and boron-containing analogues where N- and B-atoms are placed in a para-position relative to each other, in the so-called piperazine configuration.

The insertion of a heteroatom changes the structure of the transition state and the mechanism of chemisorption. An analysis of the results of quantum chemical calculations showed the highest exothermic dissociative adsorption of the H₂ molecule on B-containing graphene-like ones. For N-containing PAM, the exothermicity of the mentioned reaction is somewhat lower, for it a possibility of desorption of atomic hydrogen desorption the surface of the latter with subsequent recombination in the gas phase has been also shown. At the same time, for models of pure graphene-like layer, the data obtained indicate the impossibility of chemisorption of molecular hydrogen. Without a complete analysis of the results for all the possible locations of the pair of hydrogen atoms (formed due to dissociation of the H₂ molecule) bound by nitrogen-containing polyaromatic molecules, it can be noted that the dissociative chemisorption of the H₂ molecule, regardless of the nature of heteroatom in the PAM, is thermodynamically more probable at the periphery of the model molecules than that in their centers.

Keywords: dihydrogen, graphene-like matrix, sorption, doping with N and B-atoms, density functional theory method, Grimme's dispersion correction

INTRODUCTION

To date, due to the depletion of fossil energy resources, molecular hydrogen is increasingly considered as an alternative, renewable, energy carrier [1, 2]. However, the transition to promising hydrogen energy is impossible without the development of reliable methods of extraction, transportation and storage of hydrogen in large quantities [3, 4]. For efficient and safe storage of hydrogen one of the most promising methods is its adsorption on carbon materials [5]. Among the adsorbents that are most suitable for the physical adsorption of molecular hydrogen are carbon nanofibers, carbon nanotubes and graphene derivatives [6, 7].

Carbon nanofibers (CNF) are layered graphite nanomaterials. Sorption capacity for hydrogen at room temperature of unmodified CNF reaches only 0.7 wt. % at a high pressure of

about 10 MPa [8]. To increase the capacity for hydrogen it is used different methods of pre-treatment and modification of CNF. Thus, the activation of CNF by water vapor leads to a significant increase in their specific surface area (from 116 to 1758 m²/g). Their sorption capacity for hydrogen can be increased to 3.5 wt. %, which corresponds to the coverage of 60 % of the surface of CNF with hydrogen (77.3 K, 0.65 MPa).

Currently, the most promising carbon materials for hydrogen storage include carbon nanotubes (CNT) [9–11], systems with a high density of micropores, which are folded sheets of graphene. The π electron system of the outer wall of the CNT is characterized by a lower degree of conjugation compared to flat graphene and, consequently, a lower adsorption potential of the surface relative to the physical sorption of molecular hydrogen. On the contrary, the inner

walls have a higher adsorption potential - the adsorption centers of the inner surface of CNT are characterized by a fairly high energy of physical sorption (up to 30 kJ/mol). This is due to the overlap of the potential fields of the opposite walls of the CNT due to the very small size of the micropores, which increases the interaction energy with the adsorbed molecules in comparison with the flat surface.

Today, for the sorption of hydrogen using single-walled and multi-walled CNT, a significant disadvantage of which is the use of cryogenic conditions for physical adsorption. In single-walled nanotubes, the hydrogen capacity at atmospheric pressure reaches ~ 5 wt. % at 77 K and < 1 wt. % at room temperature and high pressure, and when using multi-walled nanotubes – 2.27 wt. % at 77 K and 0.3 wt. % at room temperature. For the CNT sample with a specific surface area of 2560 m²/g a hydrogen capacity of 4.5 wt. % was experimentally achieved at 77 K. It should be noted that the maximum possible surface area of CNT is 2630 m²/g, which corresponds to the bilateral surface coverage of graphene sheet.

Interest in the study of the interaction of hydrogen with carbon nanostructures has increased significantly with the advent of graphene, because for single-layer graphene any atom interacting with it can be considered as adatom. This interest is caused by two main reasons: first, at a certain concentration of hydrogen adatoms in the system there is a semimetal-semiconductor transition (a gap opens in the graphene spectrum); secondly, graphene is promising from the point of view of hydrogen energy as a convenient object for hydrogen storage [12–14].

The aim of this work is to elucidate the regularities of interaction of hydrogen molecules with models of graphene-like planes in which several carbon atoms are replaced by atoms that have different electronegativity from C atoms, in particular nitrogen atoms (higher electro-negativity) ones or boron (lower electronegativity) were selected.

RESEARCH METHODS

All calculations are performed using the GAMESS (US) program [15] by the theory of density functional theory (DFT) with the exchange-correlation functional B3LYP [16, 17] and the basis set 6-31G (d, p).

To account for the dispersing contributions to the energy of intermolecular complexes formation [18, 19], which stipulate the formation of supramolecular structures, the dispersion correction by Grimme – D3 [20, 21] was applied.

The choice of the DFT method with the functional B3LYP-D3 is due to the fact that its application will require less time compared to the calculations in which the functionals B97D or wb97XD are used, with that, as evidenced by literary data [22], all three functionals give similar results regarding geometric parameters and binding energy for objects that are similar to those examined in the work.

As the models for graphene nanoparticles, polyaromatic molecules (PAM) of the pyrene (Fig. 1 a), coronene (Fig. 1 b) and a molecule of a larger composition C₅₄H₁₈ (Fig. 1 c) are taken. Boron- and nitrogen-containing pyrene analogues had similar structures (Fig. 1 d, e). In order to study the effects of the nitrogen or boron atoms on the adsorption of hydrogen by the above-mentioned structures, where two carbon atoms are replaced by heteroatoms (because the B- and N- atoms have an odd number of electrons, therefore for the preservation of the general system it is necessary to introduce two atoms into the graphene).

For coronene molecule it is possible to introduce heteroatoms in different positions. The necessary models for further calculations have been chosen when comparing the total energy of the most probable models of N- and B-containing graphene-like particles. According to the results of optimization of the spatial structure of N-containing analogues of coronene molecule, the structures of which are depicted in Fig. 2 a, b, c: total energies are –954.5289692 (a), –954.5110171 (b) and –954.5344694 a.u. (c). A comparison of the total energy of three nitrogen-containing analogues has proved that the lowest value will be for the molecule in which the nitrogen atoms are placed in a *para*-position relative to each other (NN1-4 coronene), in the so-called piperazine configuration (see Fig. 2 c). For the B-containing analogues of the coronene molecule, there is a similar case – the lowest total energy (–889.9057155 a.u.) inherent the structure in which the boron atoms are in *para*-position relative to each another (BB1-4 coronene), (Fig. 2 f). The other two structures (Fig. 2 d, e) are energetically less likely (–889.8934244 and –889.8717995 a.u.).

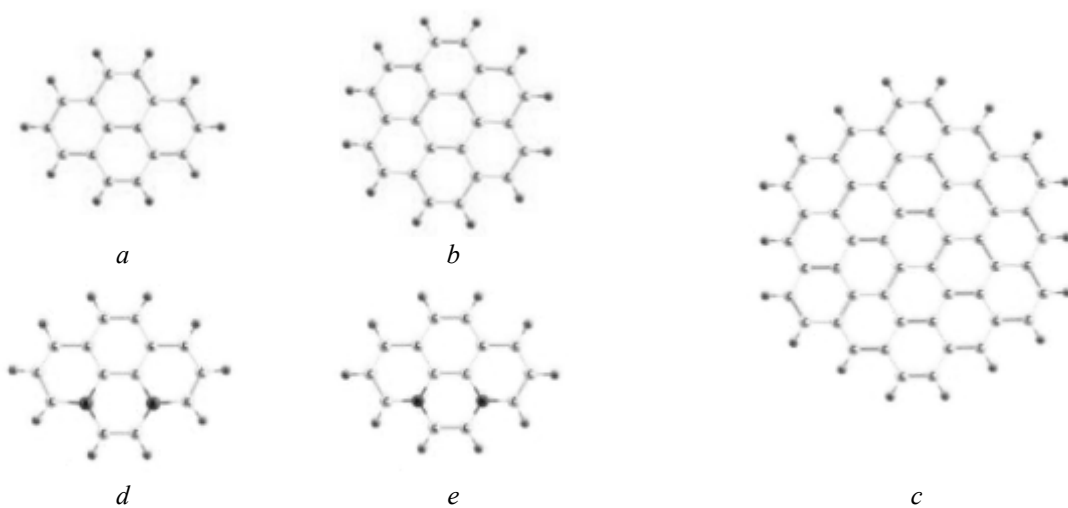


Fig. 1. Molecules of pyrene (*a*), coronene (*b*) and PAM C₅₄H₁₈ (*c*); B- and N-containing (*d*, *e*) analogues of pyrene, which simulate graphene nanoparticles with heteroatoms

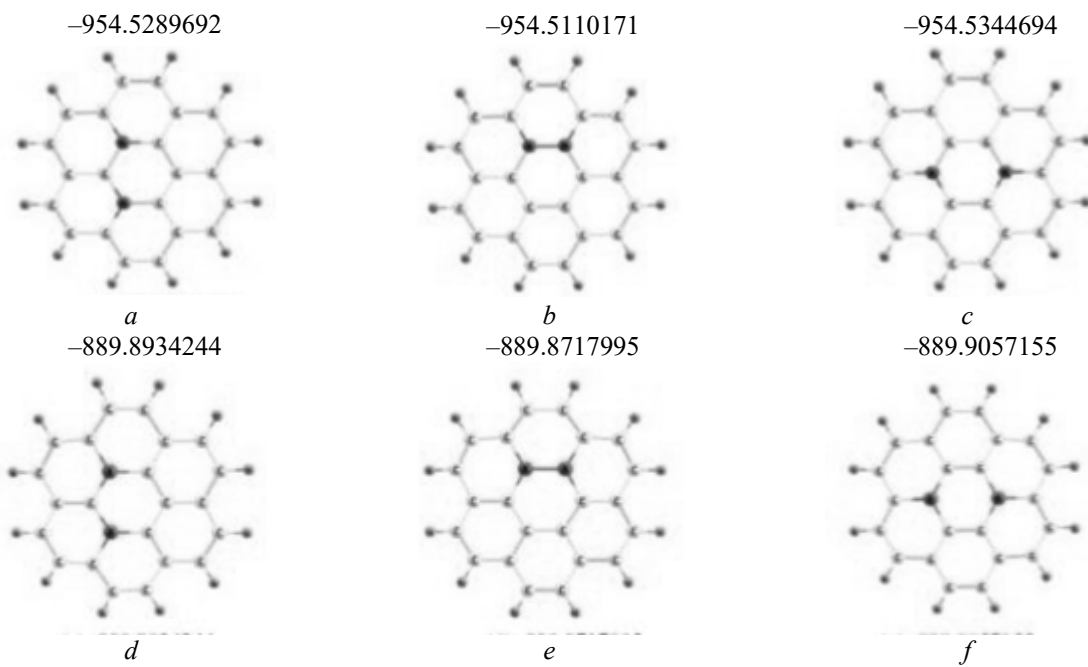


Fig. 2. 1–4 coronene analogues: nitrogen-containing NN (*a*, *b*, *c*) and boron-containing BB (*d*, *e*, *f*)

Therefore, in the subsequent calculations these models of graphene planes were used, i.e. ‘NN1-4 coronene’ and ‘BB1-4 coronene’ molecules. In addition, to take into account the impact of the dimensional effect and places of localization of the atoms of nitrogen or boron on energy of molecular hydrogen adsorption with models of graphene planes, except for the above described (Fig. 2), the carbon PAM of larger size containing 52 C-atoms and several of their

nitrogen and boron counterparts with different position of heteroatoms have been involved.

N-atoms were placed both in the central part of the PAM C₅₂N₂H₁₈ (Fig. 3 *a*) and at its periphery (Fig. 3 *b*). According to the calculations for the model in which the nitrogen atoms are located in the center, the total energy is lower (-2089.4305039 a.u.) than that for the model in which the nitrogen atoms are at the periphery (-2089.4112309 a.u.). Realistically, heteroatoms

can be placed both in the center of the graphene plane and closer to the periphery, so it is important to investigate the adsorptive capability of molecular hydrogen in the two models mentioned.

By analogy with the N-containing models, the B-containing PAM were also built. The total energy of the B-containing structure with the boron atoms in the center, as well as in the previous case, is lower (-2030.0269163 a.u.), than in the structure with the boron atoms at the periphery (-2030.0069518 a.u.).

The equilibrium spatial structure of reagents molecules, product reactions, and the

configuration of transitional states were found to minimize the gradient norm of total energy. The stationarity of the points that correspond to the lows of the optimized structures proved the absence of negative eigenvalues of the Hesse' matrices (matrices of power constants), while the presence of transitional states was confirmed by the existence of the transitional vector (*iv*), according to theorem of Marrell-Leidler [23]. The correspondence between the structures of pre-reactional complex, transitional state and reaction products is set by the internal reaction coordinate (IRC) method [24].



Fig. 3. PAM $C_{52}N_2H_{18}$ with different localization (allocated by ovals) of the atoms of the nitrogen (or boron): *a* – in the central part of the molecule, *b* – at its periphery

Calculation of physical adsorption energy ($\Delta E_{ph.ads.}$) of H_2 molecules from the gas phase was conducted according to formula (1):

$$\Delta E_{ph.ads.} = E_{ph.ads.compl.} - (E_{surf.} + E_{H2}), \quad (1)$$

where $E_{ph.ads.compl.}$ – total energy of a complex with physically adsorbed molecule H_2 , $E_{surf.}$ and E_{H2} – total energy of graphene-like cluster and hydrogen molecules respectively.

Hydrogen chemisorption energy was considered in the framework of two approaches. According to the first one, when examining the mechanism of dissociative chemisorption H_2 , this energy was defined as the energy reaction effect ($E_{react.}$) by the formula (2). This value takes into account the energy of breakdown of H-H bond and stabilization contribution, due to formation of two new C-H bonds:

$$\Delta E_{react.} = E_{ch.ads.compl.} - E_{ph.ads.compl.}, \quad (2)$$

where $E_{ch.ads.compl.}$ is the total energy of a complex with the chemically adsorbed molecule H_2 . In addition, the so-called total energy of

chemisorption, defined as energy released in the interaction of H_2 molecules from the gas phase with graphene-like clusters ($\Delta E_{ch.ads.}$), is similar to that from the formula (1):

$$\Delta E_{ch.ads.} = E_{ch.ads.compl.} - (E_{surf.} + E_{H2}). \quad (3)$$

The activation energy of the reactions ($E_{act.}$) was defined as the difference between the values of the full energy of transition state and the complex of physically adsorbed molecule H_2 ($E_{ph.ads.compl.}$):

$$E_{act.} = E_{TS} - E_{ph.ads.compl.}, \quad (4)$$

where E_{TS} is the total energy of a transitional state between the states with a physically and chemically adsorbed H_2 molecule.

RESULTS AND DISCUSSION

Physical adsorption of molecular hydrogen on the graphene-like plane. As a result of optimization of the spatial structure, physical adsorption complexes of hydrogen molecules with pyrene molecule and its N- and B-containing

analogues are localized. They are similar to each other, namely, in all intermolecular complexes, the H₂ molecule is perpendicular to the graphene plane. It is found out that the shortest intermolecular distance of C–H (2.66 Å) in the complex with pyrene, and the longest (2.89 Å) – for the complex with the boron derivative of pyrene. The calculated values of the energy of physical adsorption ($\Delta E_{ph.ads.}$) for these complexes by the formula (1) indicate that for all three cases $\Delta E_{ph.ads.}$ is almost identical and has insignificant negative value. For pyrene and its nitrogen-containing analogue it is –8.5 kJ/mol, and for boron –8.3 kJ/mol.

With increasing the size of the graphene-like plane in the adsorption complex from the pyrene to the coronene and its heteroatomic derivatives it can be seen that the spatial structure of all intermolecular complexes is similar to that of examined above. Distance C–H is somewhat shorter for all complexes with coronene molecule (0.1 Å) of similar distances in adsorption complexes with derivative pyrene, and for complexes with pyrene and coronene this value is practically the same (2.6 Å). Along with the decrease of intermolecular distances in complexes with coronene and its N-containing derivative, the energy of physical adsorption is increased by about 1 kJ/mol (–9.9 kJ/mol for the coronene and –9.8 kJ/mol for ‘NN1-4 coronene’, except for the complex with a boron-derived coronene, for which this characteristic was reduced from –8.3 to –7.1 kJ/mol).

Further increase in the size of PAM does not lead to a significant change in the structural and power parameters of the physical adsorbed complexes. The distance between H₂ molecule and PAM C₅₄H₁₈ is the same as in previously examined complexes with coronene and pyrene, and is 2.65 Å. And $\Delta E_{ph.ads.}$ is smaller on 2 kJ/mol from the similar characteristics for the coronene and is –8.1 kJ/mol.

For N-containing PAM the increase in the size from pyrene-like structure to the C₅₂N₂H₁₈ results in a monotonous slight reduction of the intermolecular distance C–H from 2.82 to 2.69 Å, which correlates with the insignificant increase of energy of physical adsorption from –8.5 to –10.0 kJ/mol. With further increase in the size of the B-containing PAM to C₅₂B₂H₁₈ intermolecular distance is not substantially increased with 2.80 to 2.87 Å. This is also the

meaning of $\Delta E_{ph.ads.}$, which is not expected increased for 1 kJ/mol to –8.2 kJ/mol.

Consequently, the analysis of the calculations of complexes with physically adsorbed hydrogen molecule has shown that the size and nature of heteroatoms in them weakly affect the physical adsorption of the hydrogen molecules on the carbon materials, however, regardless of the size of the PAM, the best hydrogen molecule physically adsorption is observed on the B-containing graphene-like material.

Dissociative chemisorption of molecular hydrogen on the graphene-like plane. With further convergence of PAM with hydrogen molecule, its chemisorption comes with the formation of chemical bonds C–H and rupture of bonds H–H, as shown for the example of pyrene (Fig. 4 a) and its derivatives with atoms of N and B (Fig. 4 b, c). The geometric parameters for all three complexes are almost the same, however it should be noted that the longest bonds C–H are in B-containing pyrene (1.119 Å) and the shortest for pyrene (1.097 Å), distances H–H for these three complexes are more than 2 Å.

Analysis of the results of calculations indicates that the values of total energy of chemisorption, obtained by the formula (3), are substantially different for these three structures. In particular, for the pyrene $\Delta E_{ch.ads.}$ is the highest (+154.1 kJ/mol). Replacement in the molecule pyrene two C-atoms on two N-atoms leads to a significant reduction in the energy of chemisorption (–74.5 kJ/mol), and for the B-containing derivative (Fig. 4 c) $\Delta E_{ch.ads.}$ is the lowest (–119.0 kJ/mol).

It is important to note that the spatial structure of the transition state for pyrene and its N- and B-containing derivatives (Fig. 5) are significantly different, indicating that nature of the heteroatom influences the mechanism of chemisorption of molecular hydrogen on the graphene-like plane.

In particular, it is found by the IRC method that during the convergence of hydrogen molecule with C-atoms of pyrene molecule, firstly one of the C-atoms of pyrene comes from the plane of pyrene molecule, changing the type of hybridization of their atomic orbitals with sp^2 on sp^3 at the distance of C–H 1.320 Å. In this case the distance between the 2nd H-atom of the H₂ molecule and the neighboring C-atom of pyrene molecule is synchronously decreasing. This C-atom is obtained from the plane of the pyrene

molecule, distance H--H continues to increase and structure is formed depicted in Fig. 5 a. Confirmation for this structure to correspond to a transitional state is the presence of a transitional vector with apparent vibrant mode with a wave number $i2412.58 \text{ cm}^{-1}$. Calculated energy activation by the formula (4) is +484.7 kJ/mol.

The energy response effect in accordance with (2) has even greater value (+162.4 kJ/mol) in comparison with the value obtained with the formula (3) $\Delta E_{ch.ads.}$ (+154.1 kJ/mol) due to the disregard energy of physical adsorption (about 8 kJ/mol).

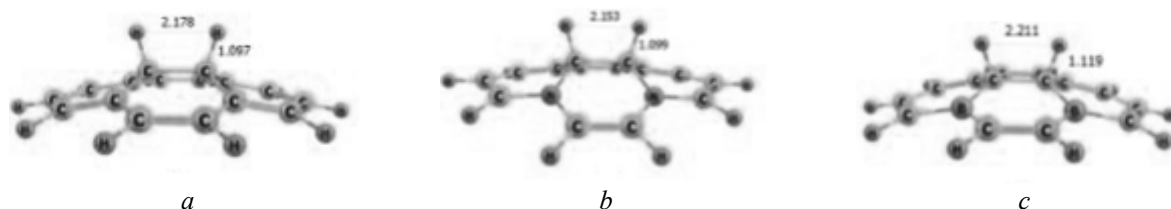


Fig. 4. Structures of the complexes of chemisorbed hydrogen molecule on pyrene molecule (a) and its N- and B-containing derivatives (b, c)

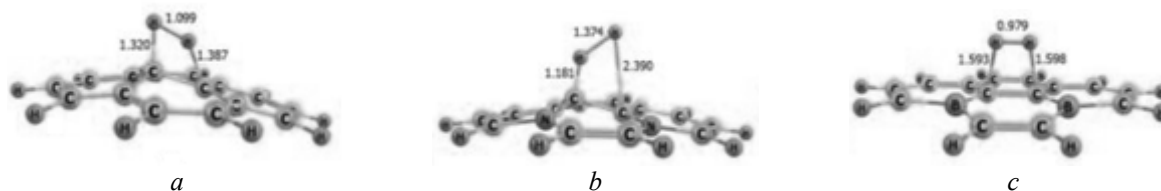


Fig. 5. The spatial structure of the complexes of transition state of chemisorption of hydrogen molecule on pyrene (a) and its N- and B-containing analogues (b, c)

Structure of the transitional state for the N-containing pyrene (Fig. 7 b) is significantly different from the previous one. It is also differed a mechanism for the chemisorption of molecular hydrogen with this PAM. Firstly, a convergence of one H-atom of H_2 molecule with one of C-atoms begins, the last comes out of the plane of pyrene molecule and at the same time the distance H--H increases. After the formation of the chemical bond C-H between not involved H-atom of H_2 and other C-atom, the formation next bond C-H begins. The corresponding transitional state is characterized by the transitional vector with the wave number $i986.98 \text{ cm}^{-1}$. The activation energy in this case is twice as lower as compared to the pyrene (+242.6 kJ/mol). The energy effect of the reaction is negative (-65.9 kJ/mol), which indicates the self-validity of this process, as opposed to the previously considered pyrene molecule.

A completely different, symmetrical structure belongs to a transition state in the interaction of molecules H_2 with B-containing analogue of

pyrene (Fig. 5 c). Peculiarities of the mechanism of chemisorption are that when approaching a hydrogen molecule along a line perpendicular to the plane of B-containing pyrene molecule in the pre-reactive complex, at the distance of C-H approximately 1.6 Å the H_2 molecule returns to 90° and is placed in parallel to the graphene plane of the derivative of pyrene. After that there is further convergence of the H-atoms of H_2 with carbon atoms with a simultaneous rupture of chemical bond into the hydrogen molecule. The activation energy for this process is the smallest of all three examined cases (+182.2 kJ/mol). However, the energy effect the reaction is also the lowest (-110.7 kJ/mol). The presence of a transitional state is confirmed by a transitional vector with a wave number $i1959.02 \text{ cm}^{-1}$.

The next step was to find out the influence of heteroatoms on the chemisorption of hydrogen molecule by increasing the size of the PAM to coronene. As with the study of physical adsorption of hydrogen molecule, for this case the

appropriate structures of N- and B-containing graphene molecules are chosen (see Fig. 2 c, f).

In case of chemisorption involving nitrogen and boron analogues of coronene it may form a significant number of different reaction products from different structure, but the same general

composition, in which two atom hydrogen can be associated with different C-atoms of carbon of model molecules. The lowest energy among them is the one in which the hydrogen atoms are attached to the C-atoms, which are adjacent to the N-atoms, as shown in Fig. 6.

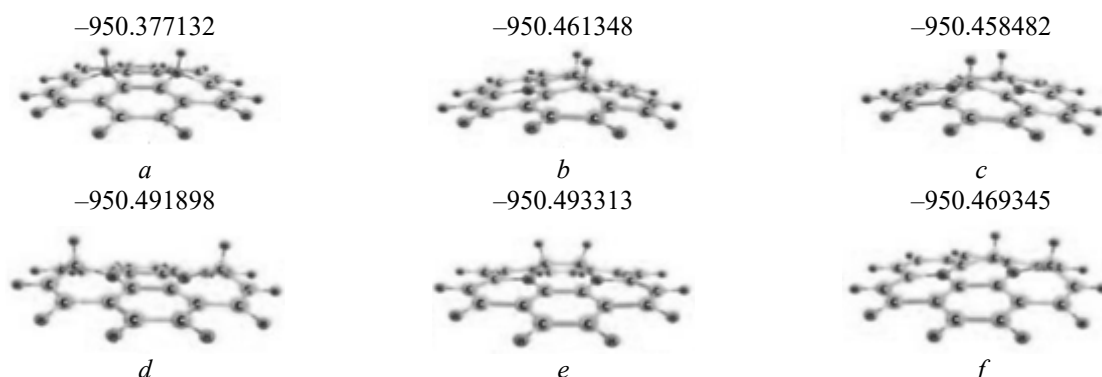


Fig. 6. The equilibrium spatial structure of the most probable complexes, formed at dissociative chemisorption of H_2 molecule on the N-containing PAM ‘NN1-4 coronene’

For B-containing PAM, similar to the previous case, the lowest energy will be for the chemisorption complex, in which the H-atoms form chemical bonds in the structure ‘BB1-4 coronene’, which is similar to the N-containing complex, shown in Fig. 6 e. Also, for comparison, it was localized chemisorption complex of coronene molecule ($\text{C}_{24}\text{H}_{12}$), in which the H-atoms form H-C bonds in such a way as it takes place in the complex depicted in Fig. 6e. Calculations according to the formula (3) for these three complexes of coronene molecule and its heteroatom-containing analogues have shown that the lowest value of $\Delta E_{ch.ads.}$ is for B-containing complex (-52.5 kJ/mol). For coronene this energy is -47.3 kJ/mol and for the N-containing analogue of coronene molecule (Fig. 6f) it is $+148.4 \text{ kJ/mol}$.

After finding out the structure of the physical and chemical adsorption systems there were localized complexes of the transition states of the reaction of the chemical interaction of molecular hydrogen with coronene and its heteroatomic derivatives. As can be seen from Fig. 7, the structure of all transition states is similar to the structure of complexes with pyrene and its heteroatomic derivatives (Fig. 5). For them, there are a wave number of transient vectors, which make up $i2476.63 \text{ cm}^{-1}$, $i1166.15 \text{ cm}^{-1}$ and $i1839.65 \text{ cm}^{-1}$, respectively.

Activation energy (482.8 kJ/mol) and the reaction energy effect ($+158.4 \text{ kJ/mol}$) are the highest for the chemisorption of H_2 on the coronene molecule. The lowest absolute values of $E_{act.}$ (224.4 kJ/mol) and $\Delta E_{react.}$ (-45.4 kJ/mol) have a place for the boron derivative ‘BB1-4 coronene’. However, it should be noted that these values are slightly higher compared to the case of pyrene ($E_{act.} = 182.2 \text{ kJ/mol}$, $\Delta E_{react.} = -110.8 \text{ kJ/mol}$). Also higher is the value of the activation energy (304.4 kJ/mol) and the energy effect of the chemisorption reaction (-37.5 kJ/mol) for ‘NN1-4 coronene’, compared with the similar parameters for the ‘BB1-4 coronene’.

In the study of the impact of the size of the graphene cluster on the energy of hydrogen chemisorption, in addition to the molecules of pyrene and coronene, the PAM of $\text{C}_{54}\text{H}_{18}$ and its N- and B-containing derivatives in which heteroatoms are placed in the center of the molecule and at its periphery (Fig. 3) were involved. In Fig. 8 the structures are given of chemisorption complexes with hydrogen molecule both in the center and closer to the periphery of the PAM.

For the structure of general composition $\text{C}_{54}\text{H}_{18}$ it is obtained the value of $\Delta E_{ch.ads.}$, which is calculated by the formula (3), indicates that regardless of the position of the chemisorbed hydrogen molecule (Fig. 8 a, d), the value of

the chemisorption energy in all cases has a positive value and is more than 100 kJ/mol (+125.5 kJ/mol for the complex in Fig. 8 *a*; +153.1 kJ/mol for the structure, which is shown in Fig. 8 *d*), which correlates with similar values $\Delta E_{ch.ads.}$ for carbon-containing PAM of

smaller size (coronene: +148.5 kJ/mol; pyrene: +154.1 kJ/mol). This indicates a low thermodynamic probability of chemisorption of the hydrogen molecule on carbon clusters under normal conditions, which is possible only at elevated temperatures.

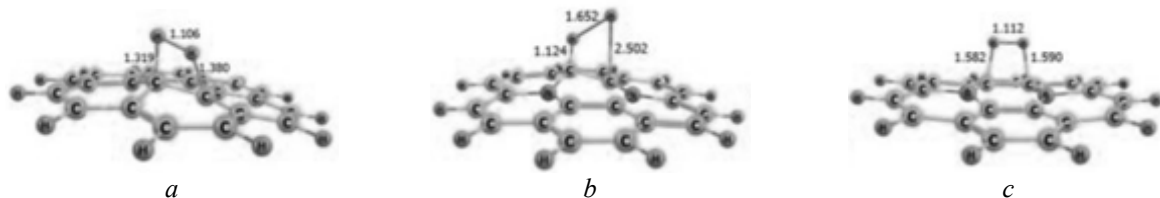


Fig. 7. Structure of the complexes of transition states of hydrogen molecule chemisorption on the coronene (*a*) and on its N- and B-derivatives (*b*, *c*)

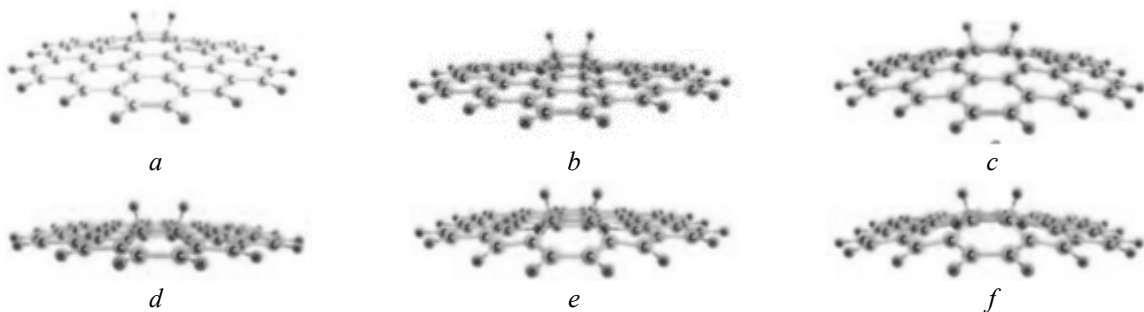


Fig. 8. The equilibrium spatial structure of chemisorption complexes as products of interactions of molecule H₂ with PAM C₅₄H₁₈ (*a* and *d*), C₅₂N₂N₁₈ (*b* and *e*) and C₅₂B₂H₁₈ (*c* and *f*)

A completely different pattern is observed for heteroatomic derivatives of PAM. In particular, for C₅₂N₂N₁₈, in which the N-atoms are located in the center of the PAM (Fig. 8 *b*), the total energy of chemisorption is +6.5 kJ/mol, and for the PAM of the same general structure, in which the N-atoms are closer to the periphery of the graphene-like cluster surface (Fig. 8 *e*), $\Delta E_{ch.ads.}$ has negative value (-35.2 kJ/mol), as in previous N-containing PAM of smaller size ($\Delta E_{ch.ads.}$ of C₁₄N₂N₁₀ = -74.5 kJ/mol, $\Delta E_{ch.ads.}$ of C₂₂N₂H₁₂) = -47.3 kJ/mol). This is evidence of the greater thermodynamic probability of chemisorption under the normal conditions of the hydrogen molecule beside the peripheral N-atoms of PAM in comparison with the central ones.

Similar to the above-examined complexes it is investigated the influence of the localization of the B-atoms in the graphene-like cluster consisting of 52 C-atoms on the total energy of chemisorption of molecular hydrogen

(Fig. 8 *c*, *f*). It has been found that regardless of the position of boron atoms in the cluster (C₅₂B₂H₁₈), $\Delta E_{ch.ads.}$ has a negative value. In this case, like in the previous two (C₅₄H₁₈ and C₅₂N₂N₁₈) cases, chemisorption at the periphery is more likely to be (-54.9 kJ/mol) than in the center of the PAM (-12.3 kJ/mol), and chemisorption energy sign coincides with those for the previously examined cases for B-containing PAM of smaller size ($\Delta E_{ch.ads.}$ of C₁₄B₂N₁₀ = -119.0 kJ/mol, $\Delta E_{ch.ads.}$ of C₂₂N₂H₁₂ = -52.5 kJ/mol).

The structures of localized complexes of transitional state depicted in Fig. 9 are similar to the above examined (Fig. 5, 7). For them, as for the previously discussed, there are also existing transitional vectors with large quantities of the wave number: *i*2679.34 cm⁻¹ for C-containing transition state, *i*1380.43 cm⁻¹ – for N-containing, and *i*1976.01 cm⁻¹ – for B-containing, respectively. This indicates that the increase in the

size of the PAM does not change the mechanism of the chemisorption of the hydrogen molecule, and the crucial for the mechanism is the nature of heteroatom within the composition of the graphene-like plane.

The calculated value of the activation energy for a boron derivative ($C_{52}B_2H_{18}$) is 270.2 kJ/mol, which is the highest compared to the previously considered boron PAM (182.3 kJ/mol for $C_{14}B_2H_{10}$, 224.4 kJ/mol for $C_{22}B_2H_{12}$). The energy effect of the $\Delta E_{react.}$ for $C_{52}B_2H_{18}$ has a negative value (-46.7 kJ/mol), which is similar to the similar value for chemisorption to 'BB1-4 coronene' (-45.4 kJ/mol), but is significantly different from $\Delta E_{react.}$ for boron pyrene (-110.8 kJ/mol). It is evident that the increase in the size of the PAM is increasing in activation

energy and decreasing the absolute value of $\Delta E_{react.}$

A slightly higher $E_{act.}$ value has been proved for chemisorption to $C_{52}N_2H_{18}$ (305.6 kJ/mol), which is almost the same as with the participation of 'NN1-4 coronene' (304.4 kJ/mol), and considerably higher than that in the case of pyrene-like N-containing cluster ($C_{14}N_2H_{10}$), for which $E_{act.} = 242.6$ kJ/mol. The energy effect of chemisorption on the $C_{52}N_2H_{18}$ is negative (-26.5 kJ/mol), which is the lowest compared with pyrene- and coronene-like PAM with N-atoms (-65.9 and -37.5 kJ/mol). Consequently (see Table), increasing the size of nitrogen-containing PAM leads to a slight increase in activation energy and to reduction of the absolute value of the energy reaction effect.

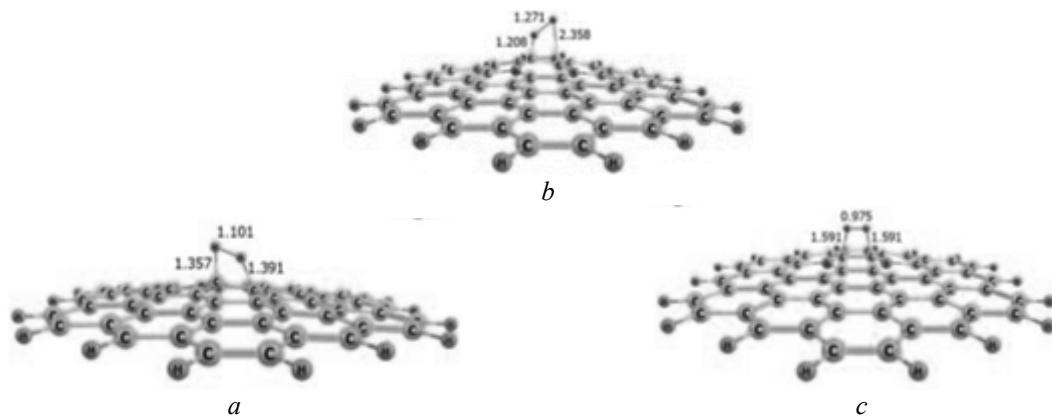


Fig. 9. Structure of the complexes of transition state of hydrogen molecule in the PAM of $C_{54}H_{18}$ (a) and its N- ($C_{52}N_2H_{18}$) and B- ($C_{52}B_2H_{18}$) derivatives (b, c)

Table. Energy of physical and chemical adsorption (in kJ/mol) of molecular hydrogen on carbon, nitrogen- and boron-containing graphene clusters, of different sizes as well as LVMO energy (in eV) for the corresponding PAM

Content of adsorbents	C			N			B		
	$C_{16}H_{10}$	$C_{24}H_{12}$	$C_{54}H_{18}$	$C_{14}N_2H_{10}$	$C_{22}N_2H_{12}$	$C_{52}N_2H_{18}$	$C_{14}B_2H_{10}$	$C_{22}B_2H_{12}$	$C_{52}B_2H_{18}$
$E(LVMO)$	-1.46	-1.40	-2.16	-1.65	-1.70	-2.20	-4.14	-4.03	-3.75
$\Delta Eph.ads.$	-8.5	-9.9	-8.1	-8.5	-9.8	-10.0	-8.3	-7.1	-8.2
$\Delta Ech.ads.$	154.1	148.4	125.5	-74.5	-47.3	-36.5	-119.0	-52.5	-54.9
$Eact.$	484.8	482.8	466.6	242.6	304.4	305.6	182.2	224.4	270.2
$\Delta E_{react.}$	162.6	158.4	133.6	-65.9	-37.5	-26.5	-110.8	-45.4	-46.7

The activation energy of the chemisorption of H_2 on $C_{54}H_{18}$ is of 466.6 kJ/mol, which is the lowest compared to the previously considered similar values for pyrene and coronene (484.8 and 482.8 kJ/mol). The same reduction in the energy effect the reaction is observed at the

chemisorption of molecular hydrogen with pyrene (162.6 kJ/mol), coronene (158.4 kJ/mol) and on the $C_{54}H_{18}$ (133.6 kJ/mol). This indicates that the increase in the size of the pure carbon graphene cluster slightly reduces the absolute value of the activation energy and the energy

response effect. However, despite the size of carbon PAM, the value of the activation energy and the energy reaction effect are the highest.

The process of interaction of hydrogen molecule with PAM can be regarded as intermolecular oxidation-reduction, in which the atoms of the PAM are reduced and hydrogen molecule are oxidized. In this case the change of degrees of oxidation of atoms of the reacting system occurs when the transfer of hydrogen atoms from the molecule of the recovery (hydrogen molecule) to the atoms of the graphene plane [25]. Therefore, if a molecule of PAM is regarded as an oxidizer, its main characteristic is the capability to join the electron density, namely the electron affinity, which according to the Koopmans' theorem [26, 27] is characterized by the energy of the lower unoccupied molecular orbitals (LUMO).

As can be seen from the Table 1, the energy of lower unoccupied orbitals correlates with the energy parameters of hydrogen molecule chemisorption.

It is found that regardless of the size of the polyaromatic molecule, for a pure carbon counterpart, the energy value of lower unoccupied molecular orbital has the smallest absolute value, and most of all - for boron-containing, indicating the largest electron-acceptor capacity, which means an oxidative capability to respect the molecule of hydrogen as a reducer.

CONCLUSIONS

Analysis of the results of quantum-chemical calculations showed exothermicity of dissociative adsorption of molecular hydrogen on N- and B-containing graphene materials. At the same time,

for pure carbon graphene layer, the calculated data indicates the low probability of chemical adsorption of molecular hydrogen on it under normal conditions.

Dissociative chemisorption of hydrogen molecules, regardless of the nature of the heteroatoms in polyaromatic molecule, is thermodynamically more likely to periphery of the model molecules than in their center.

The activation energy calculated and the energy of chemisorption of hydrogen molecule, regardless of the size of the polyaromatic molecule, is the lowest for its boron counterpart.

The energy of chemisorption of hydrogen molecule depends on the size of the model and the positions of boron and nitrogen atoms, it has negative value indicating the self-validity of the relevant process. For all examined cases, energy chemisorption parameters indicate the inefficient use of pure carbon material for chemical adsorption of molecular hydrogen in comparison with N- and B-containing ones. However, use as a reusable adsorbent hydrogen of the boron-carbon material is inappropriate, due to its considerably negative values of the energy of chemisorption, and, consequently, the irreversibility of the process of adsorption-desorption of hydrogen.

ACKNOWLEDGEMENT

The work is carried out with financial support of the target complex program of scientific researches of NAS of Ukraine "Fundamental aspects of renewable-hydrogen energy and fuel-cellular technologies" and the Contract of Employment for External Professor with Ningbo University of Technology.

Сорбція молекулярного водню на графеноподібній матриці, леговані атомами N- і B-

М.Т. Картель, В.В. Лобанов, Є.М. Демяненко, Wang Bo, А.Г. Гребенюк, О.С. Карпенко

Ningbo University of Technology

No 55-155 Cui Bai Road, Ningbo, 315016, China

Інститут хімії поверхні ім. О.О. Чуйка Національної академії наук України
вул. Генерала Наумова, 17, Київ, 03164, Україна, nikar@kartel.kiev.ua

Закономірності взаємодії молекул водню з графеноподібними площинами, в яких два атоми вуглецю заміщені атомами азоту або бору, вивчено методами квантової хімії (ТФГ, B3LYP, 6-31G**). Для врахування дисперсійних внесків в енергію утворення міжмолекулярних комплексів, що виникають під час формування адсорбційних супрамолекулярних структур, використовується дисперсійна поправка Грімме - D3. Для вивчення впливу розміру графеноподібного кластера на енергію молекулярної хемосорбції водню, використано поліароматичні молекули (ПАМ) пірену, коронену та молекула, що складається з 54 атомів вуглецю, а також їхні азот- і борвмісні аналоги, атоми N і B розміщаються в пара- положенні один до одного, у так званій конфігурації піперазину.

Введення гетероатома змінює структуру перехідного стану та механізм хемосорбції. Аналіз результатів квантово-хімічних розрахунків показав найвищу екзотермічну дисоціативну адсорбцію молекули H₂ на B-вмісних графеноподібних молекулах. Для N-вмісних ПАМ екзотермічність згаданої реакції дещо нижча, для них також показана можливість десорбції атомарного водню з їхніх поверхонь з подальшою рекомбінацією в газовій фазі. У той же час для моделей чистого графеноподібного шару одержані дані вказують на неможливість хемосорбції молекулярного водню. Без повного аналізу результатів для всіх можливих місць розташування пари атомів водню (утворених завдяки дисоціації молекули H₂), коли вони пов'язані азотвмісними поліароматичними молекулами, можна зазначити, що дисоціативна хемосорбція молекули H₂, незалежно від природи гетероатома в РАМ, є термодинамічно більш вірогідною на периферії модельних молекул, ніж у їхньому центрі.

Ключові слова: молекулярний водень, графеноподібна матриця, сорбція, допування атомами N та B, метод теорії функціоналу густини, дисперсійна поправка Grimme

REFERENCES

1. Niaz S., Manzoor T., Pandith A.H. Hydrogen Storage: Materials, Methods and Perspectives. *Renewable Sustainable Energy Rev.* 2015. **50**: 457.
2. Uyar T.S., Beşikci D. Integration of hydrogen energy systems into renewable energy systems for better design of 100 % renewable energy communities. *Int. J. Hydrogen Energy*. 2017. **42**(4): 2453.
3. Qi J., Zhang W., Cao R. Solar-to-Hydrogen Energy Conversion Based on Water Splitting. *Adv. Energy Mater.* 2018. **8**(5): 1701620.
4. Ross D.K. Hydrogen storage: The major technological barrier to the development of hydrogen fuel cell cars. *Vacuum*. 2006. **80**(10): 1084.
5. Nagar R., Vinayan B.P., Samantaray S.S., Ramaprabhu S. Recent advances in hydrogen storage using catalytically and chemically modified graphene nanocomposites. *J. Mater. Chem. A*. 2017. **5**: 22897.
6. Rajaura R.S., Srivastava S., Sharma P.K., Mathur Sh., Shrivastava R., Sharma S.S., Vijay Y.K. Structural and surface modification of carbon nanotubes for enhanced hydrogen storage density. *Nano-Structures & Nano-Objects*. 2018. **14**: 57.
7. Arjunan A., Viswanathan B., Nandhakumar V. Nitrogen-incorporated carbon nanotube derived from polystyrene and polypyrrole as hydrogen storage material. *Int. J. Hydrogen Energy*. 2018. **43**(10): 5077.
8. Chambers A., Park C., Baker R.T.K., Rodriguez N.M. Hydrogen Storage in Graphite Nanofibers. *J. Phys. Chem. B*. 1998. **102**(22): 4253.
9. Murata K.K., Kaneko K., Kanoh H., Kasuya D., Takahashi K., Kokai F., Yudasaka M., Iijima S. Adsorption mechanism of supercritical hydrogen in internal and interstitial nanospaces of single-wall carbon nanohorn assembly. *J. Phys. Chem. B*. 2002. **106**(43): 1132.
10. Gayathri V., Geetha R. Hydrogen adsorption in defected carbon nanotubes. *Adsorption*. 2007. **13**: 53.

11. Dillon A.C., Jones K.M., Bekkedal T.A., Kiang C.-H. Storage of hydrogen in single-walled carbon nanotubes. *Nature*. 1997. **386**(6623): 377.
12. McKay H., Wales D.J., Jenkins S.J., Verges J.A., de Andres P.L. Hydrogen on graphene under stress: Molecular dissociation and gap opening. *Phys. Rev. B*. 2010. **81**: 075425.
13. Lee H., Ihm J., Cohen M.L., Louie S.G. Calcium-decorated graphene-based nanostructures for hydrogen storage. *Nano Lett.* 2010. **10**(3): 793.
14. Ao Z.M., Peeters F.M. High-capacity hydrogen storage in Al-adsorbed graphene. *Phys. Rev. B*. 2010. **81**: 205406.
15. Schmidt M.W., Baldridge K.K., Boatz J.A., Elbert S.T. General atomic and molecular electronic structure system. *J. Comput. Chem.* 1993. **14**(11): 1347.
16. Becke A.D. Density-functional thermochemistry. III. The role of exact exchange. *J. Chem. Phys.* 1993. **98**(7): 5648.
17. Lee C., Yang W., Parr R.G. Development of the Colle-Salvetti correlation-energy formula into a functional of the electron density. *Phys. Rev. B*. 1988. **37**: 785.
18. Jackson K., Jaffar S.K., Paton R.S. Computational organic chemistry. *Annu. Rep. Prog. Chem., Sect. B: Org. Chem.* 2013. **109**: 235.
19. Hutchison G.R., Ratner M.A., Marks T.J. Intermolecular Charge Transfer between Heterocyclic Oligomers. Effects of Heteroatom and Molecular Packing on Hopping Transport in Organic Semiconductors. *J. Am. Chem. Soc.* 2005. **127**(48): 16866.
20. Grimme S., Ehrlich S., Goerigk L. Effect of the damping function in dispersion corrected density functional theory. *J. Comput. Chem.* 2011. **32**(7): 1456.
21. Grimme S. Density functional theory with London dispersion corrections. *Wires Comput. Mol. Sci.* 2011. **1**(2): 211.
22. Alrawashdeh A.I., Lagowski J.B. The role of the solvent and the size of the nanotube in the non-covalent dispersion of carbonnanotubes with short organic oligomers—a DFTstudy. *RSC Adv.* 2018. **8**: 30520.
23. Wales D.J., Berry R.S. Limitations of the Murrell–Laidler theorem. *J. Chem. Soc. Faraday Trans.* 1992. **88**: 543.
24. Fukui K. The path of chemical reactions - the IRC approach. *Acc. Chem. Res.* 1981. **14**(12): 363.
25. Dreyer D.R., Park S., Bielawski C.W., Ruoff R.S. The chemistry of graphene oxide. *Chem. Soc. Rev.* 2010. **39**: 228.
26. Koopmans T. Über die zuordnung von wellenfunktionen und eigenwerten zu den einzelnen elektronen eines atoms. *Physica*. 1934. **1**(1–6): 104.
27. Bellafont N.P., Illas F., Bagus P.S. Validation of Koopmans' theorem for density functional theory binding energies. *Phys. Chem. Chem. Phys.* 2015. **17**: 4015.

Received 05.05.2021, accepted 01.06.2021